Pharm Res (2012) 29:2477–2488
DOI 10.1007/s11095-012-0777-6

RESEARCH PAPER

Effect of Direction (Epidermis-To-Dermis and Dermis-To-Epidermis) on the Permeation of Several Chemical Compounds through Full-Thickness Skin and Stripped Skin

Takeshi Oshizaka • Hiroaki Todo • Kenji Sugibayashi

Received: 30 November 2011 / Accepted: 11 May 2012 / Published online: 24 May 2012

ABSTRACT

Purpose Compound permeation through stratum corneum-stripped skin is generally greater than that through full-thickness skin. In addition, epidermis-to-dermis permeation profile should be the same as dermis-to-epidermis permeation profile. However, stripped skin permeability of some compounds was lower than full-thickness skin permeability and different permeabilities were found for some compounds between the two directions of skin permeation. The reasons for these findings were investigated in this study.

Methods Full-thickness or stripped hairless rat skin was set in a Franz-type diffusion cell, and a solution of compound was applied on the epidermis or dermis side to determine the *in vitro* skin permeability.

Results Although the stripped skin permeability of pentyl paraben (PeP) with extremely high log$K_{o/w}$ was lower than full-thickness skin permeabilities, the addition of 3% ethanol resulted in the expected permeation order. Epidermis-to-dermis permeation of PeP through full-thickness skin was higher than dermis-to-epidermis permeation. Epidermis-to-dermis permeations of fluorescein isothiocyanate dextran (FD-4) and isosorbide 5-mononitrate with negative log$K_{o/w}$ were also higher than those in the opposite direction.

Conclusions Morphological observation of skin after FD-4 permeation suggested that a conically shaped trans-follicular permeation pathway model could be advocated to explain the difference between the epidermis-to-dermis permeation and that in the opposite direction.

T. Oshizaka • H. Todo • K. Sugibayashi (✉)
Faculty of Pharmaceutical Sciences, Josai University
1-1 Keyakidai
Sakado, Saitama 350-0295, Japan
e-mail: sugib@josai.ac.jp

KEY WORDS conical pore permeation model · hair follicle · interfacial resistance · permeation direction · skin permeation

INTRODUCTION

Many topical formulations containing many pharmaceutical additives in addition to therapeutically active compounds have been designed. Since such additives may have undesirable effects, skin permeation studies are very important for safety evaluation as well as effectiveness assessment. Measurement of skin permeability has been found to be difficult in *in vivo* experiments as well as *in vitro* experiments using human skin. The latter is due to the low availability and high variability of human skin. Many researchers have used hairless rat skins and pig skins owing to the high correlation between compound or chemical permeations through these skins and those through human skin (1–5). Although animal experiments have been widely undertaken, the concept of animal welfare and the 3Rs of animal experiments limit these experiments and necessitate alternatives (6–9). Understanding the skin permeation properties and the mechanism of action of compounds and chemical compounds is very important to establish alternatives to animal experiments.

Most of the permeation profiles of compounds through skin reflect kinetic processes that can be explained by Fick's law of diffusion. Generally, the uppermost layer of skin, stratum corneum, is the biggest barrier against compound entry through the skin (10–13). Since the stratum corneum consists of several layers of dead cells, corneocytes, transporters and metabolic enzymes were thought to contribute little to the skin permeation of most compounds. Thus, material permeation through full-thickness skin should be lower than that through stratum corneum-stripped skin. In addition, epidermis-to-dermis permeation should be the

same as dermis-to-epidermis permeation, even though the outer and inner surfaces are quite different as most likely is the interaction between the permeant and these two different biological tissues. In our preliminary experiments, the stripped skin permeability of some compounds was lower than the full-thickness permeability and different permeabilities of some compounds were found between the two directions of skin permeation. Parabens (methyl, ethyl, *n*-propyl, *n*-butyl, and *n*-pentyl parabens), isosorbide 5-mononitrate (ISMN), and fluorescein isothiocyanate dextran (FD-4) were used as model penetrants. Full-thickness and stripped skin samples excised from male hairless rats were used as skin membrane. Several *in vitro* skin permeation studies were conducted using Franz-type diffusion cells to evaluate diffusion and permeation profiles through the skin and to obtain morphological information on the permeation pathway.

Theory of Skin Permeation

Figure 1a and b illustrate concentration-distance profiles of compounds applied through full-thickness skin and stripped skin, respectively, in a steady state condition. Full-thickness skin consists of stratum corneum layer and underlying epidermis and dermis, which can be expressed by a 2-layered diffusion model, whereas stripped skin alone can be expressed by a one-layered diffusion model (14–16). Since the stratum corneum is the biggest barrier to the skin permeation of chemical compounds, as mentioned above, the permeation rate through full-thickness skin (Fig. 1a) is generally lower than that through stripped skin (Fig. 1b).

Figure 1c and d show a comparison of diffusion models of epidermis-to-dermis permeation (Fig. 1c) and dermis-to-epidermis permeation (Fig. 1d), where Fig. 1c is the equivalent of Fig. 1a. Unless no skin adsorption, no skin metabolism, and no transporter-mediated permeation occur in passive skin permeation, epidermis-to-dermis permeation should be exactly the same as dermis-to-epidermis permeation of chemical compounds.

Let us explain that the epidermis-to-dermis permeation through full-thickness skin is the same as the dermis-to-epidermis permeation. The abscissa in Fig. 1 shows the direction of the membrane permeation, and the width of the skin shows the thickness of the skin, whereas the axis of the ordinate represents the concentration of the penetrant applied on the skin. Hatched areas in the figures show the amount of penetrants in unit area of skin (usually presented as $\mu g/cm^2$), and products of concentration slopes in the stratum corneum and viable epidermis/dermis (*i.e.* concentration gradient) and diffusion coefficient of compounds become the permeation rate of compounds through the membrane. Two examples (one is a lipophilic compound and the other is a hydrophilic compound) are shown to explain that no difference is found between the epidermis-to-dermis and the dermis-to-epidermis permeation rates. When the partition coefficient of a lipophilic compound from the vehicle to stratum corneum is 4.0 and that from the vehicle to viable epidermis and dermis is unity (1.0), the partition coefficient from the stratum corneum to the viable epidermis/dermis must be 1/4, and that in the opposite direction is 4.0. In addition, the resistant ratio of stratum corneum against full-thickness skin is considered to be 0.8 (resistant ratio of viable epidermis and dermis against full-thickness skin is 0.2). Furthermore, compound concentration in the vehicle is considered to be 1.0, and sink condition is maintained in the receiver side. Then, the concentration gradient of penetrant across the stratum corneum becomes $16/5/L_{sc}$ and that across the viable epidermis and dermis is $1/5/L_{ved}$ for both directions, as illustrated in Fig. 1c and d. Thus, the same skin permeation rates must be obtained for the two directions since the concentration gradient is the same.

Let us explain in case of a hydrophilic compound having a partition coefficient from the vehicle to stratum corneum is 2.0 and that from the vehicle to viable epidermis and dermis is unity (1.0) as the same as above, the partition coefficient from the stratum corneum to the viable epidermis/dermis become 1/2, and that in the opposite direction is 2.0. The resistant ratio of stratum corneum against full-thickness skin is considered to be 0.95 (resistant ratio of viable epidermis and dermis against full-thickness skin is 0.05). The same compound concentration in the vehicle (1.0) applied under a sink condition in the receiver side. Then, the concentration gradient of penetrant across the stratum corneum becomes $19/10/L_{sc}$ and that across the viable epidermis and dermis is $1/20/L_{ved}$ for both directions, as illustrated in Fig. 1e and f. Thus, the same skin permeation rates must be obtained for the two directions for a hydrophilic compound.

In the case of stripped skin permeation both for a lipophilic compound and hydrophilic compound, a one-layered model is applied to explain the permeation profile. Thus, it is easy to understand that the epidermis-to-dermis permeation should be the same as the dermis-to-epidermis permeation.

In contrast, the steady state concentration for a lipophilic and hydrophilic compound in skin in the case of epidermis-to-dermis permeation is 0.33 and 0.1275 and that in dermis-to-epidermis permeation is 0.97 and 0.9725, respectively, when the thicknesses of stratum corneum and viable epidermis/dermis are 1 and 9. Thus, skin concentration differs between the cases of epidermis-to-dermis permeation and dermis-to-epidermis permeation both for lipophilic and hydrophilic compounds. Even when the other ratios were used, the calculated epidermis-to-dermis permeation of compounds must be the same to the dermis-to-epidermis permeation, but full-thickness skin concentration of the compounds after application to the dermis side is not the same to that to the epidermis side.

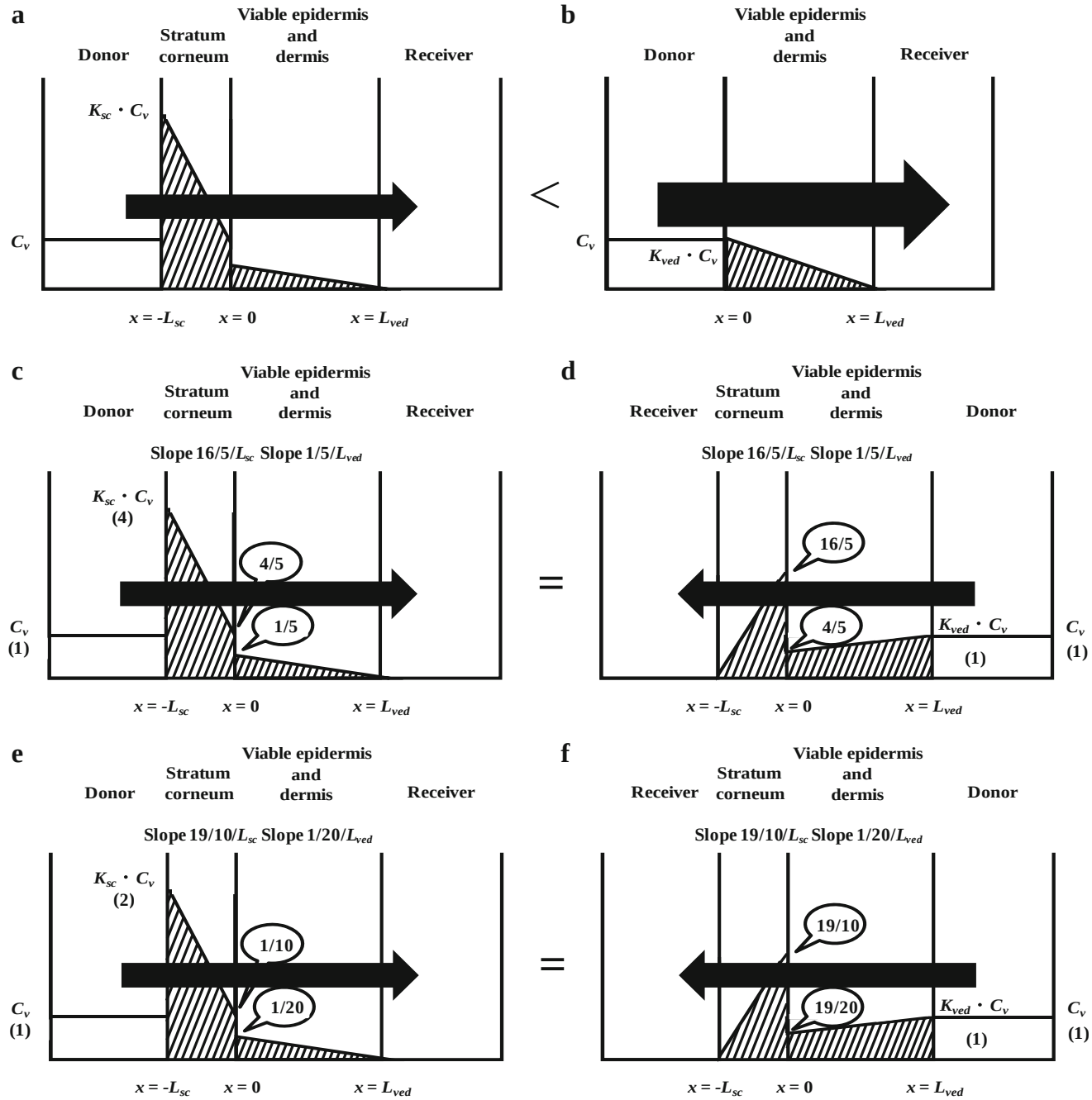

Fig. 1 Concentration-distance profile showing permeation profiles of compound through full-thickness skin (**a**) and stripped skin (**b**), and that showing full-thickness skin permeation profiles of a lipophilic and hydrophilic compound in epidermis-to-dermis (**c**, **e**) and dermis-to-epidermis directions (**d**, **f**). Width of arrows corresponds to skin permeation rate.

MATERIALS AND METHODS

Reagents and Materials

Model penetrants: methyl paraben (MP), ethyl paraben (EP), *n*-propyl paraben (PP), *n*-butyl paraben (BP), *n*-pentyl paraben (PeP), and isosorbide 5-mononitrate (ISMN), were purchased from Tokyo Chemical Industry Co., Ltd. (Tokyo, Japan). Fluorescein isothiocyanate dextran with an average molecular weight of 4.4 kDa (FD-4) was obtained from Sigma Aldrich (St. Louis, MO, U.S.A.). Table I shows a summary of molecular weights (*M.W.*) and logarithmic values of *n*-octanol/water partition coefficients ($\log K_{o/w}$) of these model compounds. Diisopropyl fluorophosphate (DFP), an esterase inhibitor, was obtained from Wako Chemical Industries, Ltd. (Osaka, Japan). Other chemicals and reagents were

of special grade or HPLC grade commercially obtained and used without further purification.

Experimental Animals

Male hairless rats (WBN/IL-Ht strain) weighing 220 to 260 g were obtained from Life Science Research Center, Josai University (Sakado, Saitama, Japan), or Ishikawa Experimental Animal Laboratories (Fukaya, Saitama, Japan). The rats were kept in an animal room where the temperature was maintained at 25±2°C and light was on from 7:00 to 19:00. Food and water were provided *ad libitum*. All animal feeding and experiments were approved by the Institutional Animal Care and Use Committee of Josai University.

Human scalp was purchased from Biopredic International (Rennes, France). The donor was a 60-year-old Caucasian lady. The average thickness of the skin was 4 mm. This human experiment was approved by and followed the guidelines on the ethical use of human-origin organs and tissues of KAC Co., Ltd. (Ritto, Shiga, Japan).

In Vitro Skin Permeation Experiments

Abdominal skin was cleaned using wet Kimwipe and excised from hairless rats under anesthesia by *i.p.* injection of pentobarbital (50 mg/kg). Stripped skin was made by stripping off the stratum corneum 20 times using adhesive tape and excised. To decrease the variability in skin permeability due to abdominal sites of skin, only right and left upper abdominal skin was used. The excess fat was trimmed off from the excised skin, and the skin sample was set in a Franz-type diffusion cell (effective diffusion area, 1.77 cm^2) in which the receiver chamber was warmed at 32°C. Compound solution and PBS were added to the cap cell and receiver cell, respectively, in all permeation experiments. Skin piece was mounted in the diffusion cell with the epidermis side facing upwards in the epidermis-to-dermis permeation experiment, whereas the dermis side facing upwards in the dermis-to-epidermis permeation experiment. DFP in pH7.4 phosphate-buffered saline (PBS) at a concentration of 2.7 μmol/mL (6 mL) was added to the receiver chamber and maintained for 30 min to reduce metabolism of parabens. Then, the skin permeation experiments were started. No effect of DFP was confirmed on the skin permeation of parabens and other compounds (17–19). In the cases of other penetrants, only PBS was used for pretreatment. A penetrant solution in PBS or 3% ethanol (0.5 or 1.0 mL) was added to the donor chamber, whereas DFP in PBS (0.54 μmol/mL) or PBS alone (6 mL each) was added to the receiver chamber to start the permeation experiments. The concentration of each penetrant applied was as follows: MP, 1520 μg/mL; EP, 500 μg/mL; PP, 200 μg/mL; BP, 100 μg/mL; PeP, 50 μg/mL; FD-4, 1 mg/mL; and ISMN, 100 mg/mL. Receiver solution was agitated using a stirrer bar and a magnetic stirrer throughout the experiments. An aliquot (500 μL) was withdrawn from the receiver chamber and the same volume of PBS was added to the chamber to keep the volume constant. Penetrant concentration in the receiver chamber was determined by HPLC or using a fluorescence spectrophotometer.

Hair on the human scalp was carefully cut using scissors. The resulting scalp was cleaned using PBS and set in a Franz-type diffusion cell. Skin permeation experiment was carried out after 12-h hydration with PBS.

Table I Physical Properties of Model Compounds

	MP	EP	PP	BP	PeP	FD-4	ISMN
M.W.	152.2	166.1	180.2	194.2	208.3	4400	191.1
$\log K_{o/w}$ [a]	1.93	2.27	2.81	3.53	4.10	−0.773	−0.151

[a] *n*-Octanol/water partition coefficient at 37°C

Determination of Extraction Ratio

The withdrawn sample containing parabens (200 μL) was mixed with 200 μL acetonitrile containing internal standard (EP for MP, MP for EP, BP for PP, PP for BP, and BP for PeP) and centrifuged at 4°C for 5 min. The obtained supernatant was injected into an HPLC system. The HPLC system (Shimadzu, Japan) consisted of a system controller (CBM-20A), a pump (LC-20 AD), an auto-sampler (SIL-20 AC), a column oven (CTO-20A), a UV detector (SPD-M20A), and analysis software (LC Solution). The column was LiChroCART® 250–4 (KGaA, 64271; Merck, Darmstadt, Germany) maintained at 40°C. Mobile phases were as follows: MP and EP, 0.1% phosphoric acid:acetonitrile (65:35); PP and BP, 0.1% phosphoric acid:acetonitrile (55:45); and PeP, 0.1% phosphoric acid:acetonitrile (45:55). The flow rate was adjusted to 1.0 mL in each case. The injection volume of sample was 20 μL and detection was carried out at UV 260 nm.

The ISMN sample was mixed with the same volume of acetonitrile and centrifuged as explained above. An absolute calibration method was used. The column was Inertsil® ODS-34.6 mm×150 mm (GL Sciences Inc., Japan), the mobile phase was water:acetonitrile (9:1), and detection was carried out at UV 220 nm. Other methods are the same as above for the paraben assay.

FD-4 was determined using a fluorescence spectrophotometer (RF-5300PC; Shimadzu, Japan) at the emission and excitation wavelengths of 490 and 520 nm, respectively.

Sectioning of Frozen Skin

Skin sectioning was done only after permeation experiment FD-4. After the permeation experiment, the skin surface was washed twice using 1 mL of PBS on the Franz-type diffusion cell. The skin sample taken from the diffusion cell was

vertically cut at 0.2 mm thickness using a razor blade, embedded in super cryoembedding medium (Leica Microsystems, Tokyo, Japan), and frozen in dry iced isopentane. Skin slices (10 μm in thickness) were made using a cryostat (CM3050S, Leica Microsystems). Each skin slice was observed under a confocal laser scanning microscope (Fluoview FV1000 and software: FV10-ASW, Olympus, Japan).

RESULTS

Figure 2 shows the time course of the cumulative amounts of parabens that permeated through full-thickness skin and stripped skin. An esterase inhibitor, DFP, was used in the skin permeation experiments of parabens. Therefore, metabolite of parabens, *p*-hydroxybenzoic acid, was not found in the receiver cells. We then ignored the effect of metabolism of parabens on the skin permeation. It was confirmed that the use of DFP did not affect the barrier function of skin (17–19). Each profile in the figure shows the typical lag time period and following steady state flux. The slopes in case of MP and EP gradually decreased with time. This was due to a decrease in donor concentration. As expected, stripped skin permeabilities were higher than full-thickness skin permeabilities of MP to PP with log$K_{o/w}$ of 1.93 to 2.81 (Fig. 2a-c). On the other hand, the stripped skin permeation

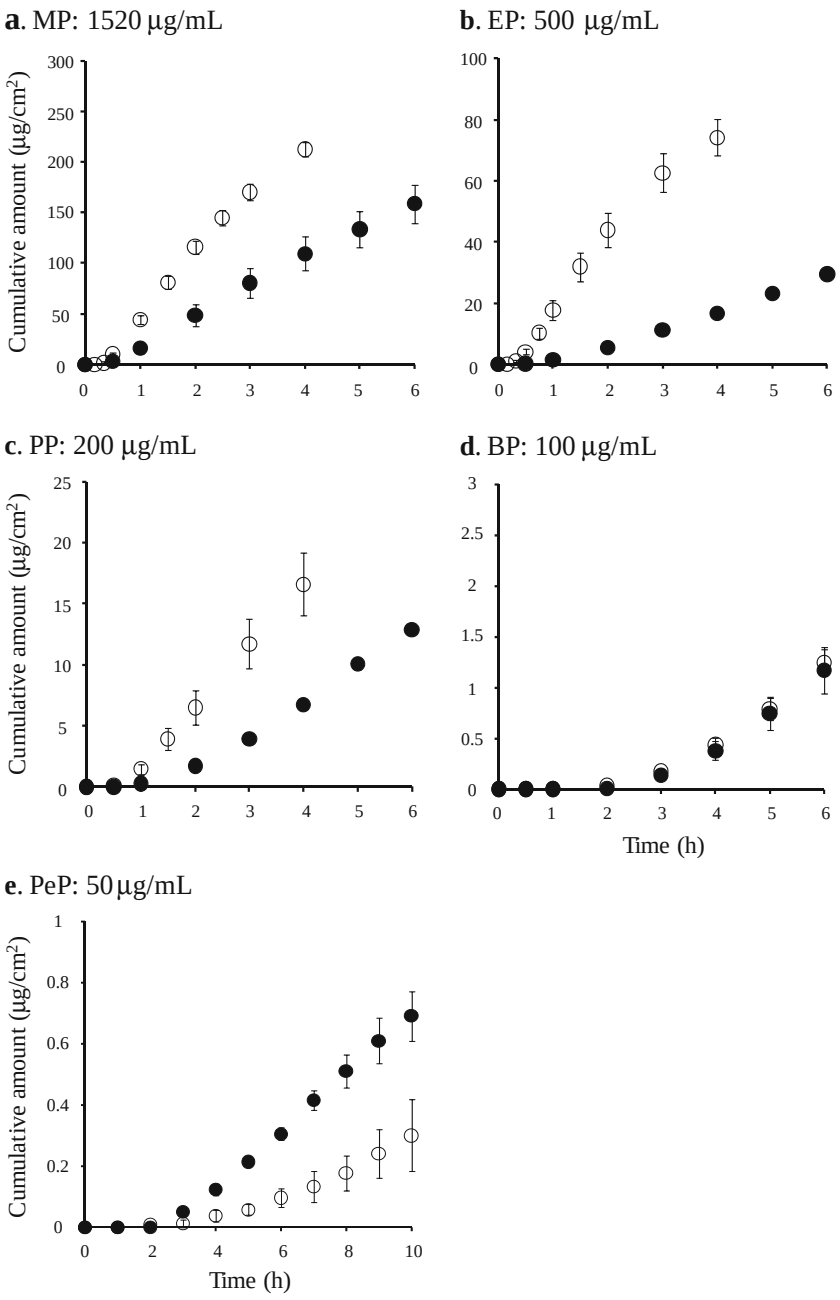

Fig. 2 Time course of changes in the cumulative amount of parabens that permeated through hairless rat skin. Symbols: through full-thickness skin from PBS (●), through stripped skin from PBS (○). Data are shown as the mean ± S.E. (*n*=3–5).

of BP ($\log K_{o/w}$, 3.53) was almost the same as the full-thickness skin permeation of the compound (Fig. 2d). Thus, low-molecular-weight compounds with a $\log K_{o/w}$ value greater than 3.53 easily permeate through the lipophilic membrane, stratum corneum, and the overall permeation is limited by the viable epidermis/dermis barrier rather than the stratum corneum barrier. Interestingly, stripped skin permeation of PeP was lower than the full-thickness skin permeation, as shown in Fig. 2e. Since the skin barrier consists of a barrier in the stratum corneum and one more barrier in the viable epidermis/dermis, almost the same permeation may be obtained for the BP permeation (Fig. 2d), but higher permeation through full-thickness skin than that through stripped skin is not possible as in PeP permeation (Fig. 2e).

We considered that this was due to interfacial migration resistance occurring or an unstirred diffusion layer forming between the bulk donor solution and the skin membrane (20–26). Theoretically, partition or distribution of penetrants immediately takes place from the vehicle to the skin at the beginning of the skin permeation (27). When interfacial resistance or unstirred layer is not negligible, the partition or distribution of penetrants from the vehicle to the skin develops a kinetic profile in the skin permeation profile. Since the effect of interfacial resistance or unstirred layer may be reduced by an increase in the affinity of skin to the donor solution, 3% ethanol was used instead of PBS. Skin permeation experiment of PeP was performed and that of MP was also carried out for comparison.

Figure 3 shows the results. MP permeations through both full-thickness skin and stripped skin from PBS were the same as those from 3% ethanol (Fig. 3a). Although ethanol was found to have an enhancing effect on the skin permeation of many compounds, 3% ethanol did not have any enhancing effect, probably due to the low concentration of ethanol. In contrast, PeP permeation from 3% ethanol through stripped skin was not significantly ($p > 0.05$) different from that through full-thickness skin (Fig. 3b), although the compound permeation from PBS had an unusual result, as shown in Fig. 2e.

As mentioned above, the use of 3% ethanol increased the affinity between the compound vehicle and the skin surface to decrease the effect of permeation resistance or an unstirred diffusion layer on the delayed skin permeation (20–26). Similar permeations of PeP ($\log K_{o/w}$, 4.1) even from 3% ethanol through stripped skin and full-thickness skin mean a greater contribution of the viable epidermis/dermis barrier to the total skin barrier.

As the main focus in the present study, the reason for the difference between epidermis-to-dermis permeation and dermis-to-epidermis permeation of compounds was evaluated. Figure 4a and b show the time course of the cumulative amount of PeP that permeated through skin from PBS and 3% ethanol, respectively. When PBS was used in the donor and receiver chambers, the epidermis-to-dermis permeation through full-thickness skin was higher than the dermis-to-epidermis permeation through full-thickness skin, epidermis-to-dermis permeation through stripped skin, and dermis-to-epidermis permeation through stripped skin. In addition, the latter three cases showed almost the same permeation. Interfacial resistance or unstirred diffusion layer may be the reason for these results (20–26). Then, 3% ethanol was used in the donor and receiver solutions, which resulted in no change in the skin permeation for the two directions.

Therefore, the interfacial resistance or unstirred diffusion layer probably affects the skin permeation of PeP. Since the PeP permeation was decreased through viable epidermis and dermis in the present study, the interfacial resistance or unstirred diffusion layer probably affects the stripped skin permeation. The reason for no interfacial effect being observed on the full-thickness skin permeation was the high affinity of PeP to the highly lipophilic stratum corneum.

Figure 5 shows the time course of the cumulative amount of MP permeated through skin from PBS and 3% ethanol solution. Almost the same stripped skin permeation of MP was observed from PBS. Through the full-thickness skin from PBS, however, the epidermis-to-dermis permeation of MP was higher than the dermis-to-epidermis permeation. Ethanol solution at a concentration of 3% was used instead

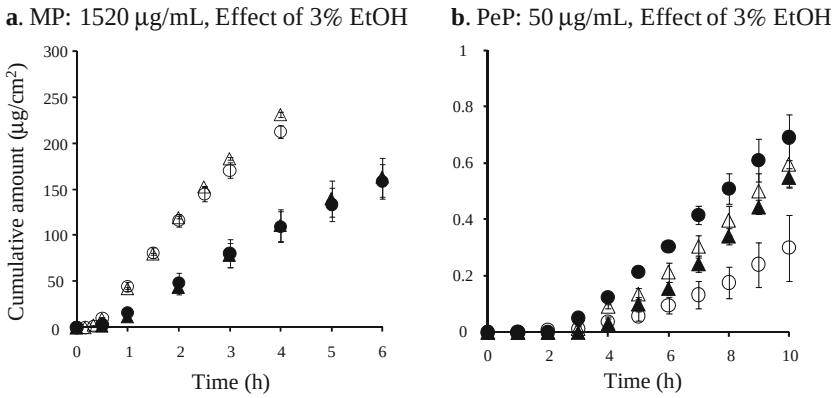

Fig. 3 Time course of changes in the cumulative amounts of MP (**a**) and PeP (**b**) that permeated through hairless rat skin. Symbols: through full-thickness skin from PBS (●), through stripped skin from PBS (○), through full-thickness skin from 3% ethanol (▲), through stripped skin from 3% ethanol (Δ). Data are shown as the mean ± S.E. (n=3–5).

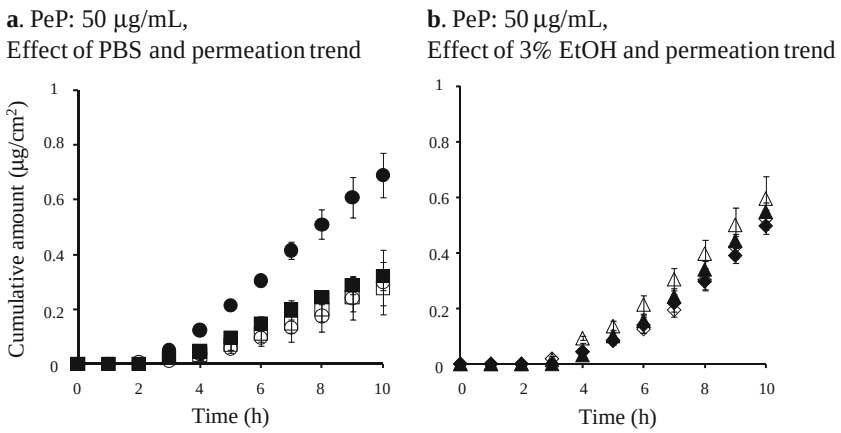

Fig. 4 Time course of changes in the cumulative amount of PeP that permeated through hairless rat skin from PBS (**a**) and 3% ethanol (**b**). Symbols: full-thickness skin permeation in the epidermis-to-dermis direction from PBS (●), stripped skin permeation in the epidermis-to-dermis direction from PBS (○), full-thickness skin permeation in the dermis-to-epidermis direction from PBS (■), stripped skin permeation in the dermis-to-epidermis direction from PBS (□), full-thickness skin permeation in the epidermis-to-dermis direction from 3% ethanol (▲), stripped skin permeation in the epidermis-to-dermis direction from 3% ethanol (Δ), full-thickness skin permeation in the dermis-to-epidermis direction from 3% ethanol (♦), stripped skin permeation in the dermis-to-epidermis direction from 3% ethanol (◊). Data are shown as the mean ± S.E. (n=3–5).

of PBS to overcome the effect of interfacial resistance or unstirred layer. The same trends (higher epidermis-to-dermis permeation through full-thickness skin) were observed. The same permeability was observed from 3% ethanol solution and PBS, suggesting that no interfacial resistance took place. Active transport or the effect of transporters could have been involved in skin permeation (28,29). However, it appears that transporters were not involved in skin permation of MP because the epidermis-to-dermis permeation through viable skin (stripped) was the same as the dermis-to-epidermis permeation. Next, the final donor concentration was determined and the permeation data were modified to take account of the adsorption of MP on the diffusion cell and skin surface (30,31). The obtained results are shown in Fig. 6. Normalized cumulative amount (% dose applied/cm^2) is used in this figure. No difference was found in the two directions of permeation of MP through full-thickness skin, suggesting that MP must be easily adsorbed or distributed on the skin surface or glass diffusion cell.

Next, the effect of direction was investigated for the skin permeation of aqueous compounds. Figures 7a and b show the time courses of the cumulative amounts of FD-4 and ISMN, respectively, which permeated through full-thickness skin. Epidermis-to-dermis permeations through stripped skin of FD-4 and ISMN were the same as dermis-to-epidermis permeations, which was similar to the case for MP (data not shown). In contrast, the epidermis-to-dermis permeations through the full-thickness skin of FD-4 and ISMN were both higher than the dermis-to-epidermis permeations. We then modified data by the final concentration in the donor solution. The results are shown in Fig. 7c and d. Normalized cumulative amount (% dose applied/cm^2) was also used for the figure the same as in Fig. 6. Different permeabilities were still observed between the epidermis-to-dermis and dermis-to-epidermis permeations.

We considered that the reason for this might be the morphological shape of the permeation pathway through skin, especially for the high-molecular-weight hydrophilic compound, FD-4. Skin permeation of chemical compounds of more than 500 Daltons is severely limited (32). Although FD-4 has a molecular weight about 9-times greater then 500

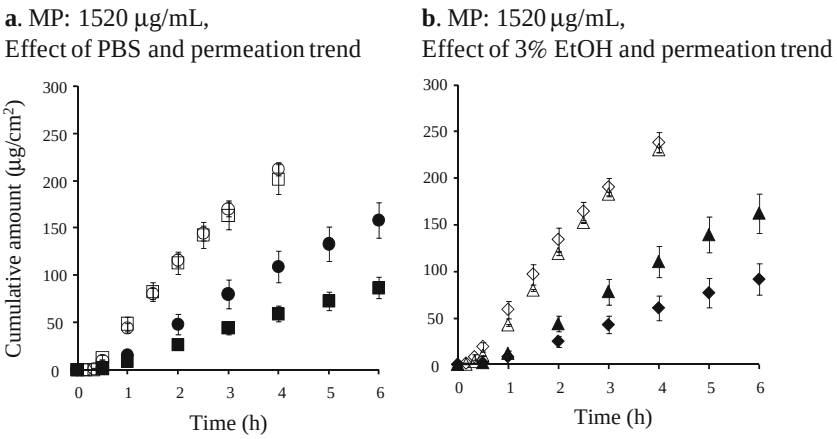

Fig. 5 Time course of changes in the cumulative amount of MP that permeated through hairless rat skin from PBS (**a**) and 3% ethanol (**b**). Symbols: as in Fig. 4. Data are shown as the mean ± S.E. (n=3).

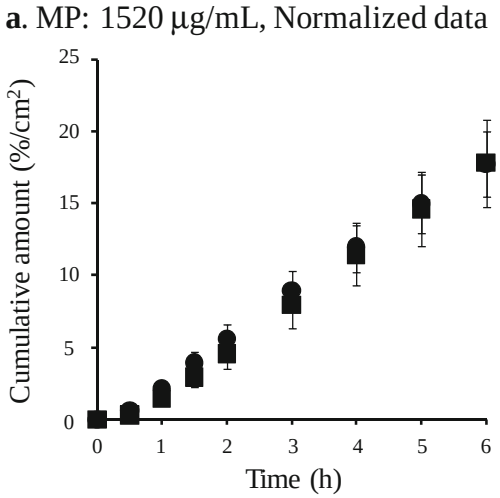

Fig. 6 Time course of changes in the normalized cumulative amount of MP that permeated through hairless rat skin. Symbols: as in Fig. 4. Data are shown as the mean ± S.E. (n=3).

Daltons, skin permeation of FD-4 was still measurable. In contrast, skin permeation of FD-4 through a three-dimensional cultured human skin model, LSE-high, could not be observed (33). This may be due to the lack of hair follicles in the cultured skin model. Figure 8 shows the morphological findings of a skin slice. The skin sample was obtained after the permeation experiment for FD-4. Figure 8a shows the skin slice after the epidermis-to-dermis permeation experiment. No fluorescence was observed in the stratum corneum, whereas low fluorescence was found in the hair follicles. On the other hand, Fig. 8b shows the view after the dermis-to-epidermis permeation experiment. No fluorescence was observed in the stratum corneum, but low fluorescence was observed in the hair follicles and viable epidermis and dermis. These results suggest that the primary permeation pathway for FD-4 must be the hair follicles. By megascopic observation (data not shown), an obvious trail of fluorescence was found on the FD-4 permeation in the sample for epidermis-to-dermis permeation, whereas no

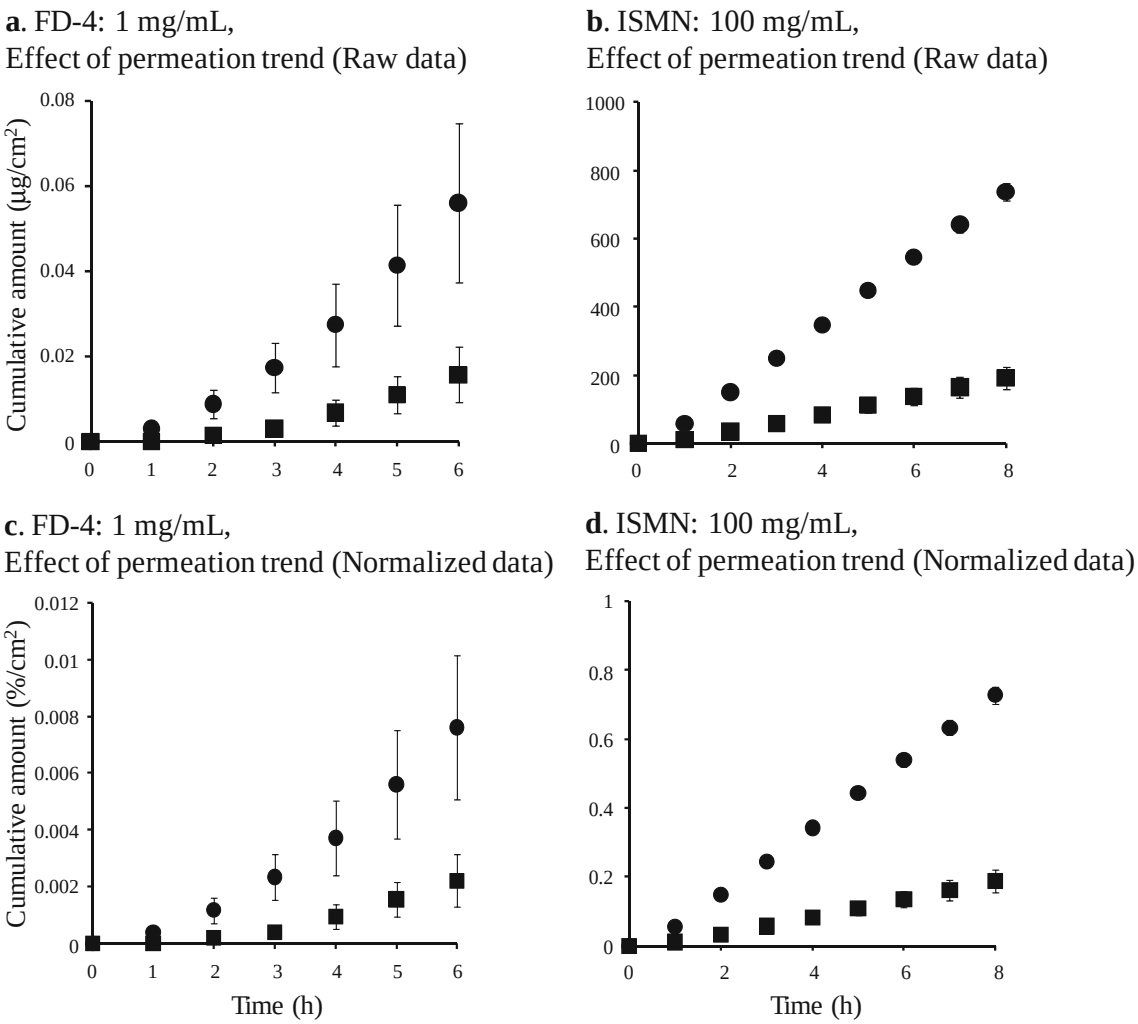

Fig. 7 Time course of changes in the cumulative amounts of FD-4 (**a**, **c**) and ISMN (**b**, **d**) permeated through full-thickness skin. (**a**, **b**) Raw data ($\mu g/cm^2$), and (**c**, **d**) normalized data (%/cm^2). Symbols: as in Fig. 4. Data are shown as the mean ± S.E. (n=3).

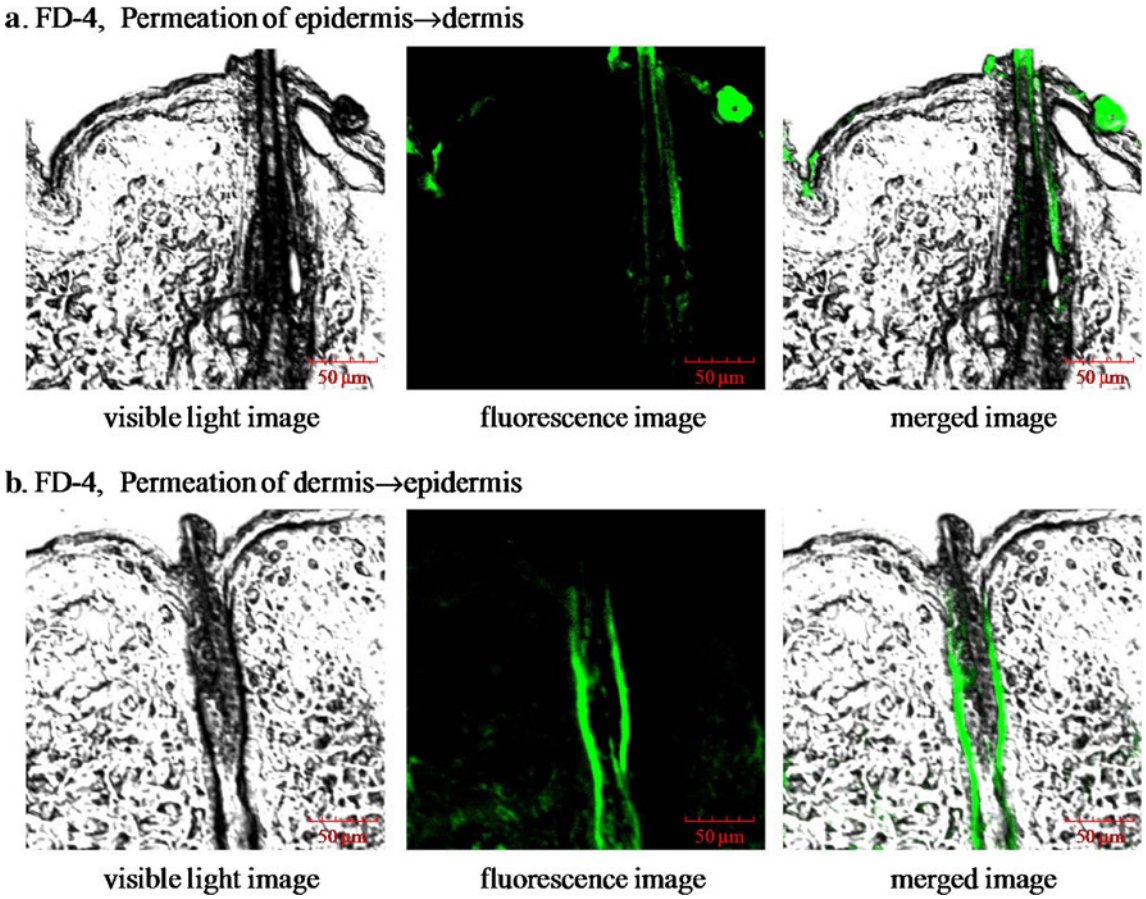

Fig. 8 Skin section image after the permeation experiment in epidermis-to-dermis (**a**) and dermis-to-epidermis directions (**b**).

clear fluorescence was observed for dermis-to-epidermis permeation. Although the dermis-to-epidermis FD-4 permeation was lower than the epidermis-to-dermis permeation, the skin concentration after application to the dermis side was much higher than that after application to the epidermis. Compounds are permeated firstly through the stratum corneum with a high resistance in the epidermis-to-dermis permeation, whereas they are permeated firstly through the dermis with a low resistance in the case of dermis-to-epidermis permeation. Therefore, the skin concentration of compounds after application to the epidermis is different from that after application to the dermis.

ISMN permeation was similar to the FD-4 permeation. Thus, hydrophilic low-molecular-weight compounds also permeate through the hair follicles. The morphological difference between the epidermis side and the dermis side, especially for the vertical shape of hair follicles, results in the difference in the skin permeation between epidermis-to-dermis and dermis-to-epidermis directions.

Figure 9 shows a comparison of ISMN permeations through human skin. Scalp human skin was used because scalp is typical skin with many hair follicles. Only one skin piece was obtained in the present study (*i.e.*, $n=1$). The dermis-to-epidermis permeation of ISMN was lower than the epidermis-to-dermis permeation, which was similar to the results for the hairless rat skin.

DISCUSSION

Since the uppermost lipophilic skin layer, stratum corneum, is the biggest barrier to the permeation of compounds through skin, skin permeation of compounds increases with lipophilicity or $\log K_{o/w}$ (8,15,34–36). However, a further increase in $\log K_{o/w}$ to more than 4.1 decreases the skin permeability (15,37,38). An increase in lipophilicity from MP to PP in the present study showed higher permeability. On the other hand, a further increase in the lipophilicity from PP to BP decreased the permeability. In addition, the stripped skin permeability was lower than that of the full-thickness skin for PeP. Furthermore, the addition of ethanol at a concentration of 3% improved the unusual results for the PeP permeation. Interfacial resistance and unstirred layer may need to be taken into account, especially for the skin permeation of highly lipophilic compounds ($\log K_{o/w}$ of more than 4.1) such as PeP.

The diffusion of chemical compounds through a dissolution-diffusion membrane is greatly affected by their

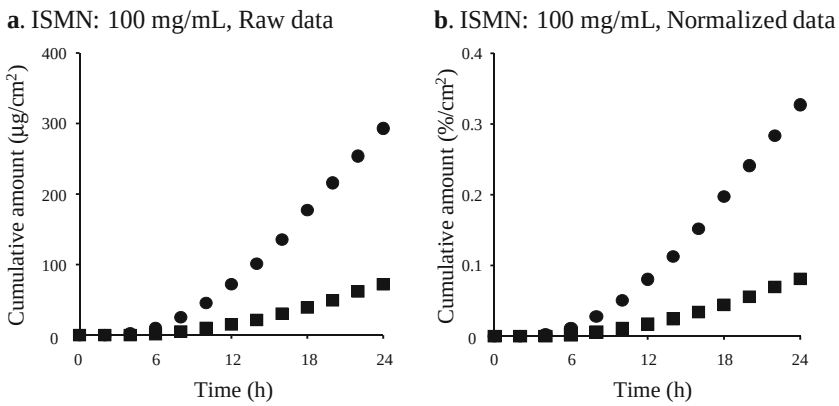

Fig. 9 Time course of changes in the cumulative amount of ISMN that permeated through human scalp skin from raw data (**a**) and normalized data (**b**). Symbols: as in Fig. 4 ($n=1$).

molecular sizes. In contrast, the distribution or partition from the donor solutions (vehicles) to the dissolution-diffusion membrane occurs rapidly, so the phenomena are not expressed by kinetics. This is well known in mass-transfer and rate process engineering (39,40). We thus used the concept of interfacial resistance to explain compound diffusion profiles from the matrices (20). No proof has been obtained as to why ethanol added to the formulations increased the skin permeation of highly lipophilic compounds. It has been proven, however, that ethanol decreases the interfacial resistance of highly lipophilic compounds between aqueous vehicles and skin (41–43). In other words, ethanol does not affect the diffusion of the compounds through the skin barrier.

Several penetrants may have adsorbed to the skin surface and diffusion cells. The adsorption took place in the epidermis-to-dermis permeation of MP for which $\log K_{o/w}$ is 1.9. The final concentration in addition to the initial concentration of penetrants must be determined to understand the real permeability. Only a few researchers are interested in dermis-to-epidermis permeation. However, comparison of epidermis-to-dermis permeation and dermis-to-epidermis permeation is very important to understand the mechanism

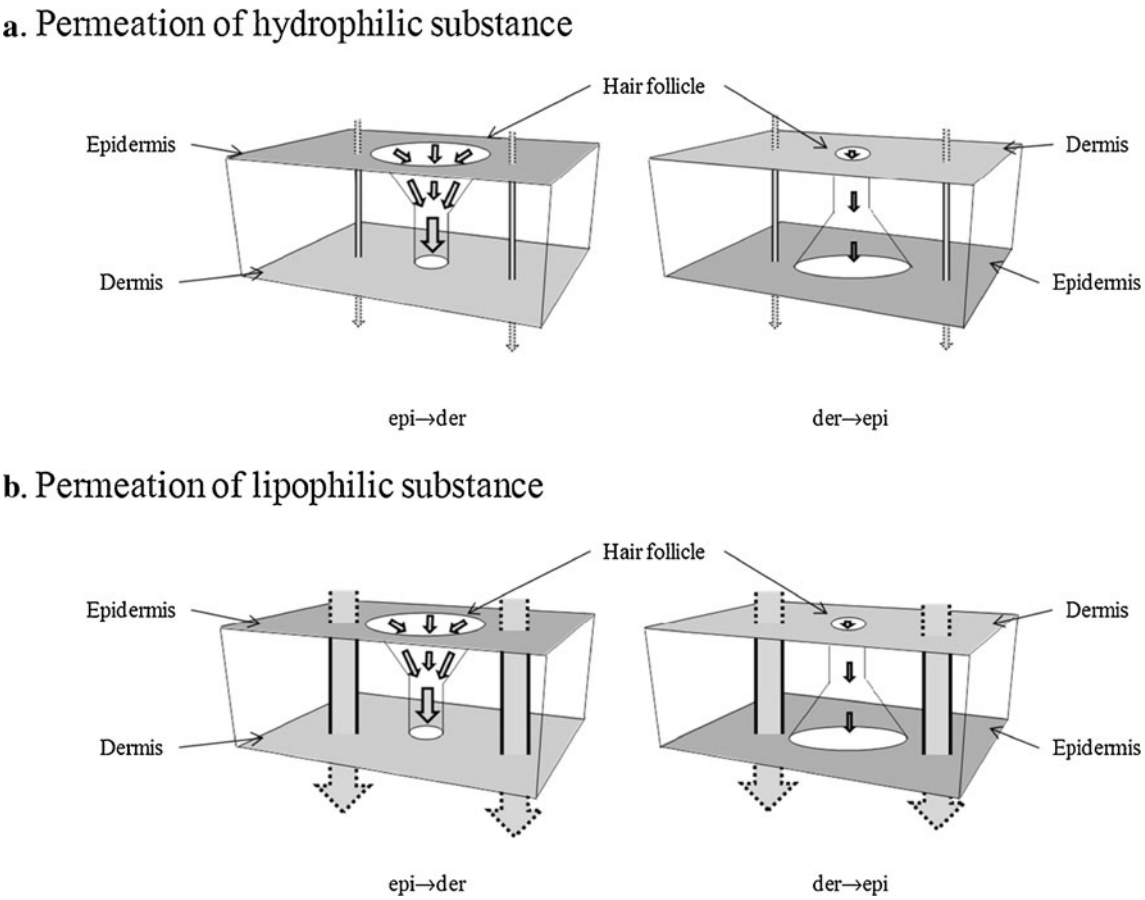

Fig. 10 Conical pore model of permeation pathway of hydrophilic compounds (**a**) and lipophilic compounds (**b**) through skin.

of skin permeation of compounds. Analysis of the adsorption of compounds is also very important. Since compounds with $\log K_{o/w}$ of about 2 are usually taken up by the skin surface, these compounds may easily adsorb to the skin.

In the case of aqueous penetrants, however, the epidermis-to-dermis permeability was higher than the dermis-to-epidermis permeability, even when modification was carried out using the final donor concentration. No or little skin permeation was observed when the molecular weight of penetrants was more than 500 Da (32). When determined in detail, scarce skin permeation was sometimes observed, even using penetrants larger than 500 Da. This is probably due to the hair follicles or other pore pathways (27,44–50). Trans-appendage routes containing the trans-follicular routes must be considered to fully understand the skin permeation profiles.

Among the compounds used in this experiment, the epidermis-to-dermis permeations of FD-4 and ISMN through full-thickness skin were different from the dermis-to-epidermis permeations. In the permeation through stripped skin, however, no effect of direction was found on the skin permeation of both hydrophilic compounds and lipophilic compounds. These findings suggest that the effect of direction on the skin permeations of FD-4 and ISMN is closely related to the vertical morphology of the stratum corneum. Figure 10 shows a schematic illustration of permeation through stratum corneum of hydrophilic compounds and lipophilic compounds. As shown in the figure, the apertural area of the appendage is largely open, and the appendage is narrower at the deeper site, suggesting a conical shape of pore for the appendage. In the case of epidermis-to-dermis permeation, the donor solution is easily approached to the large pore, resulting in the high partitioning of the penetrants into skin. When the donor solution was applied to a membrane having large pores, the compound molecules in solution contacted to large pores are easily penetrated into the pores. In contrast, in the case of dermis-to-epidermis permeation, donor solution is not easily approached to the appendage or is easily approached only to narrow appendages. Hydrophilic compounds probably permeate through the pore regions, not the real domain of the stratum corneum (Fig. 10a). Thus, the epidermis-to-dermis permeations of FD-4 and ISMN were higher than the dermis-to-epidermis permeations. Lipophilic compounds also permeate through the pore regions (Fig. 10b). The contribution of pore regions, however, is very low for the skin permeation of lipophilic compounds since the area ratio of the pore is only 0.1%.

CONCLUSION

Skin permeation profiles of high lipophilic compounds (*i.e.*, PeP) and aqueous compounds (*i.e.*, FD-4 and ISMN) were not simply explained by Fick's law of diffusion as follows: the stripped skin permeability of PeP was lower than full-thickness skin permeabilities, and the epidermis-to-dermis permeations of FD-4 and ISMN were higher than those in the opposite direction. Interfacial permeation resistance, adsorption of compounds on the skin surface and conical shape (or infundibulum) of hair follicles must be taken into account to fully understand these skin permeation profiles and mechanism involved. The present observation can be utilized to analyze transport pathway and mechanism of many penetrants through skin.

REFERENCES

1. Takeuchi H, Terasaka S, Sakurai T, Furuya A, Urano H, Sugibayashi K. Variation assessment for *in vitro* permeabilities through yucatan micropig skin. Biol Pharm Bull. 2011;34:555–61.
2. Kim MK, Lee CH, Kim DD. Skin permeation of testosterone and its ester derivatives in rats. J Pharm Pharmacol. 2000;52:369–75.
3. Obata Y, Sato H, Li CJ, Takayama K, Higashiyama K, Nagai T, Isawa K. Effect of synthesized cyclohexanol derivatives using l-menthol as a lead compound on the percutaneous absorption of ketoprofen. Int J Pharm. 2000;198:191–200.
4. Pagliara A, Reist M, Geinoz S, Carrupt PA, Testa B. Evaluation and prediction of drug permeation. J Pharm Pharmacol. 1999;51:1339–57.
5. Morimoto Y, Hatanaka T, Sugibayashi K, Omiya H. Prediction of skin permeability of drug: comparison of human and hairless rat skin. J Pharm Pharmacol. 1992;44:634–9.
6. Wilk W, Grune-Wolff B. Validity of alternatives to animal experimentation in biomedical research. Cah Anesthesiol. 1990;38:203–6.
7. Priborsky J, Muhlbachov E. Evaluation of *in-vitro* percutaneous absorption across human skin and in animal models. J Pharm Pharmacol. 1990;42:468–72.
8. Hatanaka T, Inuma M, Sugibayashi K, Morimoto Y. Prediction of skin permeability of drugs. I. Comparison with artificial membrane. Chem Pharm Bull. 1990;38:3452–9.
9. Sugibayashi K, Todo H, Oshizaka T, Owada Y. Mathematical model to predict skin concentration of drugs: toward utilization of silicone membrane to predict skin concentration of drugs as an animal testing alternative. Pharm Res. 2010;27:134–42.
10. Moser K, Kriwet K, Naik A, Kalia YN, Guy RH. Passive skin penetration enhancement and its quantification *in vitro*. Eur J Pharm Biopharm. 2001;52:103–12.
11. Elias PM. Epidermal lipids, barrier function, and desquamation. J Invest Dermatol. 1983;80:44–9.
12. Downing DT. Lipid and protein structures in the permeability barrier of mammalian epidermis. J Lipid Res. 1992;33:301–13.
13. Williams AC, Barry BW. Skin absorption enhancers. Crit Rev Ther Drug Carrier Sys. 1992;9:305–53.
14. Higuchi T. Physical chemical analysis of percutaneous absorption process from creams and ointments. J Soc Cosmet Chem. 1960;11:85–97.
15. Yamaguchi K, Mitsui T, Aso Y, Sugibayashi K. Structure-permeability relationship analysis of the permeation barrier properties of the stratum corneum and viable epidermis/dermis of rat skin. J Pharm Sci. 2008;97:4391–403.
16. Meidan VM, Pritchard D. A two-layer diffusion model for describing the variability of transdermal drug permeation. Eur J Pharm Biopharm. 2010;74:513–7.
17. Tamura M, Sueishi T, Sugibayashi K, Morimoto Y, Juni K, Hasegawa T, Kawaguchi T. Metabolism of testosterone and its

ester derivatives in organotypic coculture of human dermal fibroblasts with differentiated epidermis. Int J Pharm. 1996;131:263–71.
18. Ahmed S, Imai T, Otagiri M. Evaluation of stereoselective transdermal transport and concurrent cutaneous hydrolysis of several ester prodrugs of propranolol: mechanism of stereoselective permeation. Pharm Res. 1996;13:1524–9.
19. Sugibayashi K, Hayashi T, Matsumoto K, Hasegawa T. Utility of a three-dimensional cultured human skin model as a tool to evaluate the simultaneous diffusion and metabolism of ethyl nicotinate in skin. Drug Metabol Phamacokin. 2004;19:352–62.
20. Kokubo T, Sugibayashi K, Morimoto Y. Mathematical models describing the drug release kinetics from pressure sensitive adhesive matrix. J Contr Release. 1992;20:3–12.
21. Anissimov YG, Roberts MS. Diffusion modeling of percutaneous absorption kinetics: 2. Finite vehicle volume and solvent deposited solids. J Pharm Sci. 2001;90:504–20.
22. Hadgraft J, Ridout G. Development of model membranes for percutaneous absorption measurements. I. Isopropyl myristate. Int J Phram. 1987;39:149–56.
23. Albery WJ, Burke JF, Leffler EB, Hadgraft J. Interfacial transfer studied with a rotating diffusion cell. J C S Faraday Trans I. 1976;72:1618–28.
24. Hadgraft J. Calculations of drug release rates from controlled release devices. The slab. Int J Pharm. 1979;2:177–94.
25. Tojo K. Hydrodynamic characteristics of an *in vitro* drug permeation cell. Ind Eng Chem Fundamen. 1985;24:368–73.
26. Henning A, Schaefer UF, Neumann D. Potential pitfalls in skin permeation experiments: influence of experimental factors and subsequent data evaluation. Eur J Pharm Biopharm. 2009;72:324–31.
27. Scheuplein RJ. Mechanism of percutaneous absorption. II. Transient diffusion and the relative importance of various routes of skin penetration. J Invest Dermatol. 1967;48:79–88.
28. Li Q, Tsuji H, Kato Y, Sai Y, Kubo Y, Tsuji A. Characterization of the transdermal transport of flurbiprofen and indomethacin. J Contr Release. 2006;110:542–56.
29. Ito K, Kato Y, Tsuji H, Nguyen HT, Kubo Y, Tsuji A. Involvement of organic anion transport system in transdermal absorption of flurbiprofen. J Contr Release. 2007;124:60–8.
30. Sugibayashi K, Hosoya K, Morimoto Y, Higuchi WI. Effect of the absorption enhancer, Azone, on the transport of 5-fluorouracil across hairless rat skin. J Pharm Pharmacol. 1985;37:578–80.
31. Morimoto Y, Sugibayashi K, Hosoya K, Higuchi WI. Penetration enhancer effect of Azone on the transport of 5-fluorouracil across hairless rat skin. Int J Pharm. 1986;32:31–8.
32. Bos JD, Meinardi MM. The 500 dalton rule for the skin penetration of chemical compounds and drugs. Exp Dermatol. 2000;9:165–9.
33. Todo H, Kimura E, Yasuno H, Tokudome Y, Hashimoto F, Sugibayashi K. Permeation pathway of macromolecules and nanospheres through skin. Biol Pharm Bull. 2010;33:1394–9.
34. Potts RO, Guy RH. Predicting skin permeability. Pharm Res. 1992;9:663–9.
35. Flynn GL, Yalkowsky SH. Correlation and prediction of mass transport across membranes I: influence of alkyl chain length on flux-determining properties of barrier and diffusant. J Pharm Sci. 1972;61:838–52.
36. Lien EJ, Gao H. QSAR analysis of skin permeability of various drugs in man as compared to *in vivo* and *in vitro* studies in rodents. Pharm Res. 1995;12:583–7.
37. Yano T, Nakagawa A, Tsuji M, Noda K. Skin permeability of various non-steroidal anti-inflammatory drugs in man. Life Sci. 1986;39:1043–50.
38. Scheuplein RJ, Blank IH, Brauner GJ, MacFarlane DJ. Percutaneous absorption of steroids. J Invest Dermatol. 1969;52:63–70.
39. Quinn JA, Jeanin PG. Interfacial resistance: diffusion into a laminar liquid-liquid jet. Chem Eng Sci. 1961;15:243–50.
40. Scott EJ, Tung LH, Drickamer HG. Diffusion through an interface. J Chem Phys. 1951;19:1075–8.
41. Sugibayashi K, Nemoto M, Morimoto Y. Effect of several penetration enhancers on the percutaneous absorption Indomethacin in hairless rats. Chem Pharm Bull. 1988;36:1519–28.
42. Kim YC, Park JH, Ludovice PJ, Prausnitz MR. Synergistic enhancement of skin permeability by N-lauroylsarcosine and ethanol. Int J Pharm. 2008;352:129–38.
43. Suhonen TM, Bouwstra JA, Urtti A. Chemical enhancement of percutaneous absorption in relation to stratum corneum structural alterations. J Control Release. 1999;59:149–61.
44. Du Plessis J, Egbaria K, Ramachandran C, Weiner ND. Topical delivery of liposomally encapsulated gamma-interferon. Antiviral Res. 1992;18:259–65.
45. Feldmann JR, Maibach HI. Regional variation in percutaneous penetration of 14 C cortisol in man. J Invest Dermatol. 1967; 48:181–3.
46. Maibach HI, Feldmann JR, Hilby TH, Serat WF. Regional variation in percutaneous penetration in man. Pesticides Arch Environ Health. 1971;23:208–11.
47. Illel B. Formulation for transfollicular drug administration: some recent advances. Crit Rev Ther Drug Carrier Syst. 1997;14:207–19.
48. Wosicka H, Cal K. Targeting to the hair follicles: current status and potential. J Dermatol Sci. 2010;57:83–9.
49. Lauer AC, Lieb LL, Ramachandran C, Flynn GL, Weiner ND. Transfollicular drug delivery. Pharm Res. 1995;12:179–86.
50. Ramachandran C, Fleisher D. Transdermal delivery of drug for the treatment of bone diseases. Adv Drug Deliv Rev. 2000;42:197–223.